Wave Propagation in Helical Multi-Wire Cables

Fabien Treyssède, Laurent Laguerre

7th European Workshop on Structural Health Monitoring
July 8-11, 2014. La Cité, Nantes, France

WAVE PROPAGATION IN HELICAL MULTI-WIRE CABLES

Fabien Treyssède[1], **Laurent Laguerre**[1]

[1] *LUNAM Université, IFSTTAR, GERS, AI, Route de Bouaye, 44344 Bouguenais, France*

fabien.treyssede@ifsttar.fr

ABSTRACT

Elastic guided waves are of great interest for the inspection of elongated structures. In practice, analytical or numerical modeling tools are required for a better understanding of the propagation of guided waves, which are multimodal and dispersive, and thereby for the optimization of inspection systems. However, cables are complex structures, helical, multi-wired and highly prestressed. This further complicates the interpretation of measurement. This paper is devoted to the modeling of wave propagation inside seven-wire strands, typically encountered in civil-engineering cables. It gives an overview of recent works, mainly conducted at Ifsttar, in order to account for the helical geometry, interwire coupling and prestress in numerical models. Then, the energy transfer from the central wire to the peripheral ones is investigated by considering an excitation localized into the central wire. The numerical results allow to understand how the energy transfer can decrease with frequency as well as to discover a new compressional mode, of local type, which could be of interest for the non-destructive evaluation or the structural health monitoring of cables.

KEYWORDS : *wave, cable, simulation, curvature, prestress*

INTRODUCTION

Elastic guided waves are of great interest for the inspection of elongated structures such as cables. Guided waves are yet multimodal and dispersive, which complicates the physical interpretation of measurement. In practice, analytical or numerical modeling tools are required to optimize inspection systems.

Cables are complex structures that are difficult to model using analytical approaches. Several difficulties indeed occur. Cables are generally made of individual steel wires that are helical. The contact between wires forms a multi-wire coupled system. Besides, cables are subjected to high tensioning forces which can modify the propagation of waves. Additionally, wires are often embedded into a solid matrix (cement for instance) used for protecting steel. In this work, attention is restricted to seven-wire strands, constituted by one central cylindrical wire and six peripheral helical wires. Such a structure is typically encountered in civil-engineering cables.

This paper shows how the above-mentioned difficulties can be overcome. A so-called semi-analytical finite element (SAFE) formulation is proposed in Sec. 1.. The equilibrium equations are written in a non trivial helical coordinate system to study individual helical wires. In Sec. 2., it is shown that the proposed SAFE formulation can handle the whole seven-wire structure, although the coordinate system is different for each wire at first sight. In Sec. 3., the formulation is then extended to include the effects of axial load, which generates both prestress and predeformation. The static prestressed state is computed from a homogenization method specifically written in twisting coordinates. In Sec. 4., some simulations under excitation are perfomed on the full seven-wire model using modal expansion techniques based on SAFE eigenmodes in order to analyze the energy transfer between wires.

1. HELICAL SAFE FORMULATION

With SAFE methods, one only needs to mesh the cross-section of the waveguide [1, 2]. The initial full 3D problem is reduced to a 2D modal problem. For the analysis of helical structures, the equilibrium equations must be rewritten in a non trivial curvilinear coordinate system attached to the helix centerline [3].

1.1 Equations

This section recalls the helical SAFE formulation. Details can be found in Refs. [3,4]. (x,y) denote the cross-section coordinates while s is the axial coordinate along the helix centerline.

In the helical system, the strain-displacement relation can be written as:

$$\boldsymbol{\epsilon} = (\mathbf{L}_{xy} + \mathbf{L}_s \partial/\partial s)\mathbf{u} \tag{1}$$

where $\mathbf{L}_{xy}$ is the operator containing all terms but derivatives with respect to the s-axis:

$$\mathbf{L}_{xy} = \frac{1}{1+\kappa x}\begin{bmatrix} (1+\kappa x)\partial/\partial x & 0 & 0 \\ 0 & (1+\kappa x)\partial/\partial y & 0 \\ \kappa & 0 & \tau y\partial/\partial x - \tau x\partial/\partial y \\ (1+\kappa x)\partial/\partial y & (1+\kappa x)\partial/\partial x & 0 \\ \tau y\partial/\partial x - \tau x\partial/\partial y & -\tau & -\kappa + (1+\kappa x)\partial/\partial x \\ \tau & \tau y\partial/\partial x - \tau x\partial/\partial y & (1+\kappa x)\partial/\partial y \end{bmatrix}, \tag{2}$$

and $\mathbf{L}_s$ is the operator of s-derivatives:

$$\mathbf{L}_s = \frac{1}{1+\kappa x}\begin{bmatrix} 0 & 0 & 0 \\ 0 & 0 & 0 \\ 0 & 0 & 1 \\ 0 & 0 & 0 \\ 1 & 0 & 0 \\ 0 & 1 & 0 \end{bmatrix}. \tag{3}$$

κ and τ are the helix curvature and torsion respectively. We stress that the expressions for $\mathbf{L}_{xy}$ and $\mathbf{L}_s$ do not depend on s, which proves that guided waves truly exist in helical structures.

A SAFE approach consists in applying a time Fourier transform as well as a spatial Fourier transform along s before discretizing the cross-section (x,y) by a finite element method. Inside one finite element e, the displacement field is thus expressed as follows:

$$\mathbf{u}(x,y,s,t) = \mathbf{N}^e(x,y)\mathbf{U}^e e^{i(ks-\omega t)} \tag{4}$$

where $\mathbf{U}^e$ is the nodal displacement vector and $\mathbf{N}^e$ is the matrix of nodal interpolating functions of the element e.

The variation formulation of three-dimensional elastodynamics yields, from Eqs. (1)–(4), the following eigenvalue problem:

$$\{\mathbf{K}_1 - \omega^2\mathbf{M} + ik(\mathbf{K}_2 - \mathbf{K}_2^T) + k^2\mathbf{K}_3\}\mathbf{U} = \mathbf{0} \tag{5}$$

with the elementary matrices:

$$\begin{array}{l} \mathbf{K}_1^e = \int_{S^e} \mathbf{N}^{eT}\mathbf{L}_{xy}^T\mathbf{C}\mathbf{L}_{xy}\mathbf{N}^e\sqrt{g}dS,\ \mathbf{K}_2^e = \int_{S^e} \mathbf{N}^{eT}\mathbf{L}_{xy}^T\mathbf{C}\mathbf{L}_s\mathbf{N}^e\sqrt{g}dS, \\ \mathbf{K}_3^e = \int_{S^e} \mathbf{N}^{eT}\mathbf{L}_s^T\mathbf{C}\mathbf{L}_s\mathbf{N}^e\sqrt{g}dS,\ \mathbf{M}^e = \int_{S^e} \rho\mathbf{N}^{eT}\mathbf{N}^e\sqrt{g}dS \end{array} \tag{6}$$

where $g = (1+\kappa x)^2$, $dS = dxdy$, $\mathbf{C}$ is the matrix of material properties.

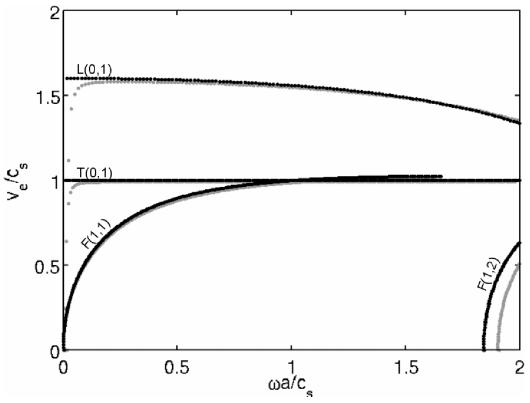

Figure 1 : Normalized energy velocity dispersion curves of isolated wires (i.e. uncoupled from eachother). Black: central cylindrical wire, gray: peripheral helical wire.

1.2 Results for individual wires

Figure 1 compares the dimensionless dispersion curves obtained for the isolated central cylindrical wire (radius a=2.7mm) and the isolated peripheral helical wire (radius $0.967a$, helix lay angle of $7.9°$) constituting a seven-wire strand. In both cases, the energy velocity is measured along a straight axis. Mechanical properties are as: E=2.17e11Pa, ν=0.28, ρ=7800kg/m^3. The normalized frequency is given by $\omega a/c_s$, $c_s = \sqrt{E/2\rho(1+\nu)}$ denoting the shear wave velocity. For clarity, the dimensional frequency here ranges from 0 to 390kHz. Minor differences are observed between both wires because the lay angle of the helical wire is small. The frequency shift of the $F(1,2)$ mode is due to the smaller radius of peripheral wire. A strong decrease of energy velocity occurs for the $L(0,1)$ and $T(0,1)$ modes at lowest frequencies inside the helical wire. The decrease of the former has been confirmed by experiments in Ref. [5].

2. WAVES IN SEVEN-WIRE STRANDS

2.1 The twisting system

A question arises about the proper invariant coordinate system to be used for a multi-wire helical waveguide, made of both straight and helical wires. The adequate system is indeed given by $\kappa = 0$ and $\tau = 2\pi/L$ where L denotes the helix pitch. Such a coordinate system is twisting along the straight axis [5]. With this system, the cross-section plane remains perpendicular to the straight axis but rotates around this axis by following peripheral wires. As the central wire is circular and isotropic, the cross-section and material properties remain translationally invariant in a twisting system. A twisting system can be viewed as a particular case of helical systems. This proves the existence of guided waves inside twisted structures such as seven-wire strands.

2.2 Results

The FE mesh of the whole strand cross-section is shown in Fig. 2. To preserve the linearity of the problem, the interwire contact conditions are assumed as perfectly stick. This is equivalent to suppose that friction is high enough to prevent any dynamic slip between wires.

Figure 3a gives the normalized energy velocity plot of the seven-wire strand. Compared to isolated wires, the dispersion curves exhibit a far more complex pattern due to interwire interactions. The figure clearly shows an apparent cut-off of the fastest mode (compressional-like $L(0,1)$ mode) around $\omega a/c_s = 0.35$, corresponding to 68kHz. This phenomenon, sometimes referred to as the 'notch frequency', coincides with experimental results of the literature [6, 7]. This apparent cut-off indeed

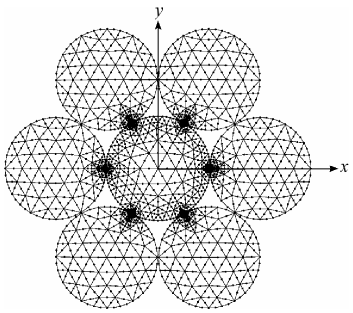

Figure 2 : Cross-section FE mesh of a seven-wire strand.

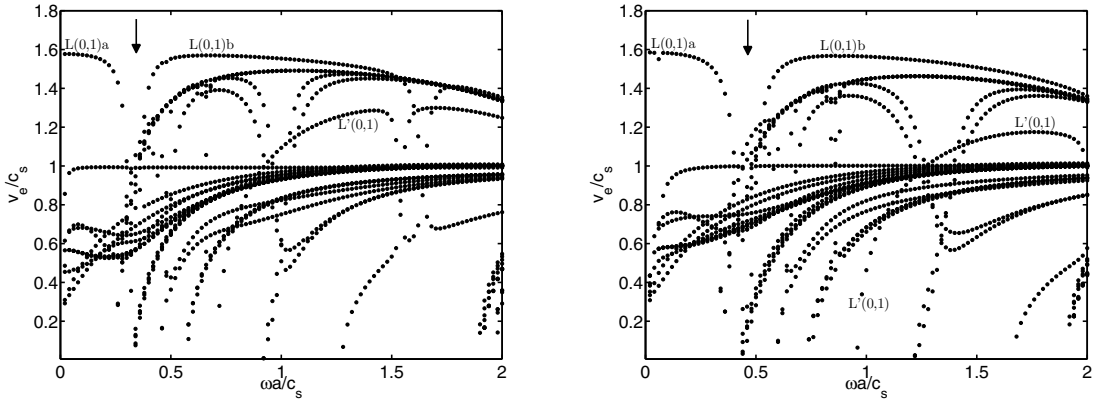

Figure 3 : Normalized energy velocity dispersion curves for the seven-wire strand, (a) unloaded and (b) loaded by a 0.6% tensile strain. The arrow indicates the notch frequency.

correspond to a sudden veering between two distinct branches [5], denoted as $L(0,1)a$ and $L(0,1)b$ in Fig. 2. Numerical tests have shown that this curve veering phenomenon is mainly due to Poisson effect, and to a less extent, to the curvature of peripheral wires. Outside the veering region, it can be noticed that the fastest compressional-like mode unexpectedly looks like the $L(0,1)$ mode of the central wire (compare Figs. 1 and 3a).

3. PRESTRESS EFFECTS

For straight waveguides, few papers have condidered prestress effects with SAFE methods [8, 9]. Finnveden [10] has proposed a circumferential SAFE formulation including preload in order to model inflated car tyres. Treyssede et al. [11] have recently extended the helical SAFE method to account for the effects of axial loads in wave propagation. This section briefly presents how axial loads can be accounted for in seven wire strands.

3.1 Equations

In the presence of prestress, the variational formulation of three-dimensional elastodynamics is modified by the following additional term, often called geometric stiffness in the literature:

$$\int_{V_0} \mathrm{tr}(\nabla_0 \boldsymbol{\delta u} \cdot \boldsymbol{\sigma}_0 \cdot \nabla_0 \mathbf{u}^T) dV_0 \tag{7}$$

$\mathrm{tr}(\cdot)$ is the trace and ∇_0 is the gradient operator with respect to the prestressed configuration. $\boldsymbol{\sigma}_0$ is the Cauchy prestress, i.e. the stress tensor associated with the prestressed state.

Applying the SAFE technique yields an eigenvalue problem having the same form as Eq. (5), but each elementary matrices $\mathbf{K}_i$ (i=1,2,3) is augmented by a term related to the geometric stiffness operator (7). Besides, the elementary matrices must now be expressed on the prestressed geometry, predeformed by axial loads.

The static prestressed state is computed from a homogenization method specifically written in twisting coordinates [12]. This allows to restrict the problem to the cross-section, as with SAFE methods. The static problem is solved by inverting a linear system of the following form:

$$\mathbf{K}_1\mathbf{U} = \mathbf{F} \tag{8}$$

where $\mathbf{K}_1$ has already been defined in Sec. 1.1 and $\mathbf{F}$ is the external load given under the form of an applied axial strain.

3.2 Results

The numerical model has been validated for helical springs in Refs. [11, 12]. Note that the preliminar study of uncoupled wires, as done without axial load, is not relevant here because the applied axial strain would tremendously predeforms an isolated peripheral wire. In a seven-wire strand, this predeformation is indeed quite small since the radial displacement of peripheral wires is constrained by the presence of the central one.

Figure 3b shows the dispersion curves obtained for the seven-wire strand subjected to an axial tensile strain of 0.6%. Compared to Fig. 3a, the notch frequency now shifts around the dimensionless frequency 0.44, corresponding to 86 kHz. This results is in good agreement with experimental results, approximately 88 kHz in Ref. [7]. Numerical experiments have shown that the phenomenon responsible for this shift is indeed the increase of contact area between the central and peripheral wires.

4. Interwire energy transfer

4.1 Calculation of the excited field

In this section, we are interested in solving the forced response problem, similar to Eq. (5) but with a non-zero excitation $\mathbf{F}(k)$ at the right hand side . This can be perfomed by expanding the solution as a sum of guided modes. Taking advantage of biorthogonality relations and applying the Cauchy residue theorem, the authors have shown in Ref. [13] that the solution as a function of $z > 0$ can be written as:

$$\mathbf{U} = \sum_{m=1}^{M} \alpha_m \frac{\mathbf{U}_m}{\sqrt{P_m}} e^{ik_m z} \tag{9}$$

with:

$$\alpha_m = \frac{i\omega}{4\sqrt{P_m}} \mathbf{U}_m^* \mathbf{F}(k_m) \tag{10}$$

where the summation in Eq. (9) is performed over positive-going modes and P_m denotes the power flow of the mth mode. The notation * is used for matrix conjuguate transpose. No viscoelastic effect is considered here. Note that the above solution neglects the contribution of non-propagating modes (M should be understood as the number of propagating modes and excludes those non-propagating) and hence constitutes a far-field approximation. Given that the power flow of a non-propagating mode is equal to zero, the near-field region, where non-propagating modes may have non-negligible contribution, is indeed of less interest for the present study.

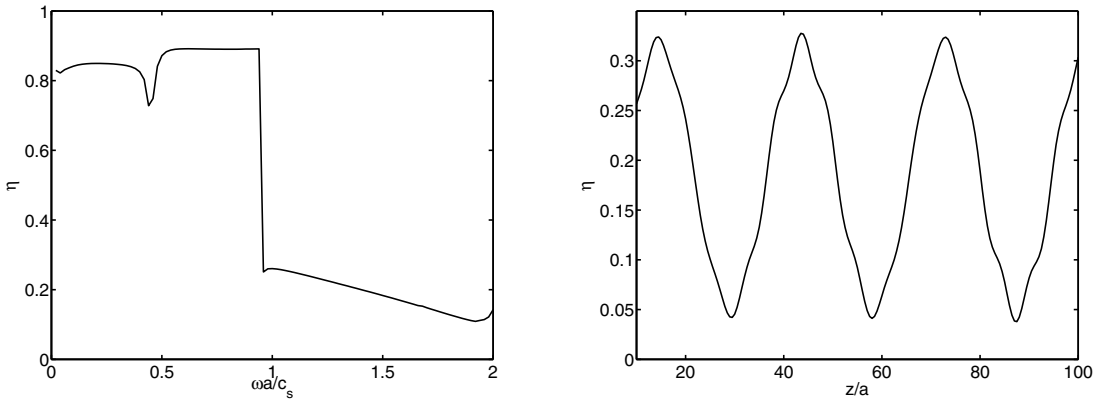

(a) (b)

Figure 4 : Energy transfer ratio η for a strand subjected to a 0.6% tensile strain, (a) as a function of the normalized frequency (η is z-averaged for each frequency) and (b) as a function of the propagation distance z/a (for $\omega a/c_s = 1.5$).

4.2 Results

One considers an excitation $\mathbf{F}$, normal to the cross-section and distributed over the cross-section of the central wire as a half-sine function vanishing at its boundary. This excitation is equal to zero over the peripheral wires. It is concentrated at $z = 0$ ($\mathbf{F}$ thus does not depend on k).

This section is focused on the transfer of energy from the central wire to the peripheral ones. The acoustic field of interest to quantify the energy transfer is the power flow. We define η, the ratio of the power flow inside the six peripheral wires to the power flow of the whole seven-wire strand:

$$\eta = 1 - \frac{P_{\text{central}}}{P_{\text{total}}} \tag{11}$$

A small η means a weak energy transfer to the peripheral wires and inversely. The power flow can be calculated from the following formula [4]:

$$P = \frac{\omega}{2}\text{Im}(\boldsymbol{\alpha}^* \mathbf{B}_u^* \mathbf{B}_f \boldsymbol{\alpha}) \tag{12}$$

where $\boldsymbol{\alpha} = [\alpha_1\ \alpha_2\ ...]^T$ is the vector of modal coefficients, $\mathbf{B}_u = [\mathbf{U}_1\ \mathbf{U}_2\ ...]$ is the basis matrix of column eigenvectors and $\mathbf{B}_f$ is the matrix of column eigenforces [4].

Figure 4a shows the ratio η as a function of frequency for a loaded strand (0.6% tensile strain). In the low frequency region $[0;1]$, the energy transfer to peripheral wires is high. This is an expected result since the $L(0,1)$-like mode of a strand has a global behavior [5] (global motion of the whole strand in the longitudinal direction). Hence, one expects to have a nearly equal repartition of power flow inside each wire, corresponding to a value of η equal to 6/7. Figure 4a is in agreement with this value in $[0;1]$. A first decrease of η is localized around the notch frequency, where it has been shown in Ref. [5] that the modeshapes associated to the $L(0,1)$-like mode strongly change (curve veering phenomenon).

Figure 4a exhibits a sudden drop of η near $\omega a/c_s = 1$. In the frequency range $[1;2]$, the energy transfer then becomes weak. This could suggest that the motion of the strand is sufficiently localized inside the central wire to be uncoupled from the other wires.

Nevertheless, as shown in Fig. 4b for a fixed frequency (here, $\omega a/c_s = 1.5$), η oscillates around an averaged value as a function of the propagation distance z. These oscillations occur with non-negligible amplitudes, which means that the energy transfer can be weak at some distance but signifi-

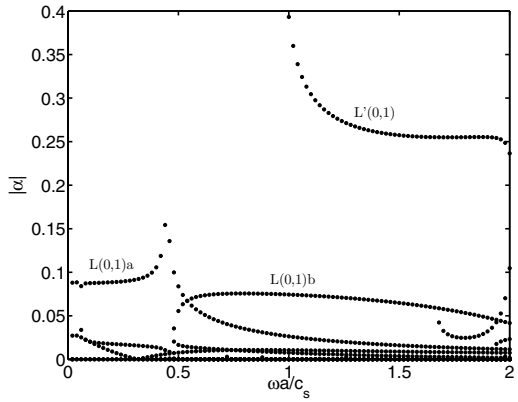

Figure 5 : Modulus of modal coefficients for a strand subjected to a 0.6% tensile strain.

cant at other ones. Such a phenomenon is likely to complicate the non-destructive evaluation (NDE) of strands. Note that Fig. 4a indeed plots the z-averaged value of η in order to get rid of this z dependence.

The sudden energy transfer drop observed in Fig. 4a can indeed be explained by the excitation of a new compressional-like mode, denoted as $L'(0,1)$, whose motion is localized in the central wire. This mode can be readily identified in Fig. 3b from its cut-off frequency, which occurs at $\omega a/c_s = 1$ and coincides with the energy drop of Fig. 4a. To confirm this explanation, Fig. 5 plots the modulus of the modal coefficients α_m of propagating modes. The power of the localized $L'(0,1)$ mode after its cut-on is clearly greater than the global $L(0,1)$ mode. This new mode could be of interest for NDE applications.

CONCLUSION

This paper has reviewed some recent findings on how to handle the helical geometry, the interwire coupling as well as the effect of high tensioning forces in the SAFE numerical modeling of seven-wire strands. Each modeling step has been validated by reference results, either analytical, numerical or experimental. The SAFE model has allowed to understand strand features such as the notch frequency phenomenon. Yet, although the finite element mesh is reduced on the two-dimensional cross-section, solving the whole 6+1 problem may lead to high computation times, which limits the application of the numerical method to low frequency (i.e. up to hundreds of kHz in practice).

Then, some simulations under excitation have been perfomed using modal expansion techniques in order to analyze the energy transfer from the central wire to the peripheral ones. The numerical results help to understand how the energy transfer can decrease with frequency. This decrease suggests that each wire could be studied separately in a higher frequency range. Besides, a new compressional mode localized in the central wire has been discovered, which could be of potential interest for the inspection of cables.

Works are in progress to account for the presence of a surrounding solid matrix, often used for protecting steel strands, by combining the SAFE method with a perfectly matched layer (PML) technique.

REFERENCES

[1] L. Gavric. Computation of propagative waves in free rail using a finite element technique. *Journal of Sound and Vibration*, 185:531–543, 1995.

[2] T. Hayashi, C. Tamayama, and M. Murase. Wave structure analysis of guided waves in a bar with an arbitrary cross-section. *Ultrasonics*, 41:175–183, 2006.

[3] F. Treyssède. Elastic waves in helical waveguides. *Wave Motion*, 45:457–470, 2008.

[4] F. Treyssède. Mode propagation in curved waveguides and scattering by inhomogeneities: application to the elastodynamics of helical structures. *Journal of the Acoustical Society of America*, 129:1857–1868, 2011.

[5] F. Treyssède and L. Laguerre. Investigation of elastic modes propagating in multi-wire helical waveguides. *Journal of Sound and Vibration*, 329:1702–1716, 2010.

[6] H. Kwun, K. A. Bartels, and J. J. Hanley. Effects of tensile loading on the properties of elastic-wave propagation in a strand. *Journal of the Acoustical Society of America*, 103:3370–3375, 1998.

[7] L. Laguerre, M. Brissaud, and J. C. Aime. Low-frequency ultrasound reflectometry device based on magnetoelastic transducers for the non destructive evaluation of steel rods and cables. *Bulletin des Laboratoires des Ponts et Chaussées*, 239:7–27, 2002.

[8] F. Chen and P. D. Wilcox. The effect of load on guided wave propagation. *Ultrasonics*, 47:111–122, 2007.

[9] P. W. Loveday. Semi-analytical finite element analysis of elastic waveguides subjected to axial loads. *Ultrasonics*, 49:298–300, 2009.

[10] S. Finnveden and M. Fraggstedt. Waveguide finite elements for curved structures. *Journal of Sound and Vibration*, 312:644–671, 2008.

[11] F. Treyssède, A. Frikha, and P. Cartraud. Mechanical modeling of helical structures accounting for translational invariance. part 2: Guided wave propagation under axial loads. *International Journal of Solids and Structure*, 50:1383–1393, 2013.

[12] A. Frikha, P. Cartraud, and F. Treyssède. Mechanical modeling of helical structures accounting for translational invariance. part 1: Static behavior. *International Journal of Solids and Structure*, 50:1373–1382, 2013.

[13] F. Treyssède and L. Laguerre. Numerical and analytical calculation of modal excitability for elastic wave generation in lossy waveguides. *Journal of the Acoustical Society of America*, 133:3827–3837, 2013.